Applied Physics A (2017) 123:774
https://doi.org/10.1007/s00339-017-1354-y

Applied Physics A
Materials Science & Processing

Au@CdO core/shell nanoparticles synthesized by pulsed laser ablation in Au precursor solution

Ayman M. Mostafa[1,2] · Samir A. Yousef[3] · Wael H. Eisa[2] · Mahmoud A. Ewaida[3] · Emad A. Al-Ashkar[1,2]

Received: 5 April 2017 / Accepted: 27 October 2017 / Published online: 15 November 2017

Abstract
Au@CdO core/shell nanocomposite was prepared using Pulsed Laser Ablation in Liquids (PLAL) via one step-process. A nanosecond pulsed laser (Nd:YAG, $\lambda = 1064$ nm) was used to ablate Cd sheet immersed in $HAuCl_4$ solution. The surface plasmon resonance (SPR) using UV–vis absorption spectroscopy was employed to monitor the fast changes occurring in the NP colloidal solutions upon interaction between Cd sheets and Au precursor. The structure of the as-prepared samples was confirmed by high resolution transmission electron microscope (HRTEM) analysis and energy dispersion X-Ray spectroscopy (EDX) analysis. A mechanism for the growth of Au@CdO core/shell nanocomposite was given.

1 Introduction

In recent years, Transition metal nanoparticles (NPs) especially noble-metal NPs have spectacular scientific interest and draw the attention of researchers in the field of nanotechnology and nanoscience. That is because in the case of nanometric size the appearing exciting novel physical and chemical properties are not present in the bulk state such as optical, catalytic, electronic, and magnetic properties [1–3]. These promising and modern properties of the metal NPs were attributed to two mechanisms. The first is the quantum confinement effect in at least one dimension on its nanoscale with respect to its bulk. The second is the increasing surface to volume ratio leading to increase the number of strained or dangling bonds at their surfaces [4].

Core/shell NPs, mixing of physicochemical properties of different metal NPs to produce new and unique properties, have attracted more attention [5]. These properties would be very useful in several fields and would open a new technology. From this fact, several metals could be mixed with the noble to produce bimetallic NPs to enhance its structure as catalytic, stability, activity, and reactivity properties of pure metal NPs [6, 7]. The effect of neighboring from different elements of NP atoms to produce bimetallic NPs in the form of either alloy structure or core/shell structure leads to unique optical properties different from its properties in isolated case [8, 9].

Gold NPs represent the most attractive noble metals because of their unique physicochemical properties, [5–7] e.g., thermal stability, no toxicity, and optical properties. Therefore, it is used in several applications as cellular drug delivery, linear and nonlinear optical (NLO) [8, 9], surface plasmon resonance (SPR), surface-enhanced Raman scattering (SERS), and biomarkers in the diagnosis of liver, lung, and breast cancer [10]. In nanofabrication field, the production Au NPs as a noble metal is widely used compared to others such as Cu or Ag. That is because of, in particular Au, the localized surface plasmon resonance (LSPR) can be tuned through visible-NIR region. So, this property is interesting for a lot of applications such as photonics and biological imaging [11].

The coupling between transition metals and noble metal NPs are thought to display amazing optical properties [12]. Cadmium oxide (CdO) NPs is a second chosen metal oxide in the bimetallic NPs due to their fascinating electrical and optical properties as they are n-type semiconductor metal oxide with a direct band gap of 2.5 eV and an indirect band gap of 1.98 eV. This property gives CdO the high absorption and emission capacity of radiation in the energy gap [13].

✉ Ayman M. Mostafa
aymanmdarwish@gmail.com

[1] Laser Technology Unit, Centre of Excellence for Advanced Sciences, National Research Center, Dokki, Cairo, Egypt

[2] Spectroscopy Department, Physics Division, National Research Center, Dokki, Cairo, Egypt

[3] Physics Department, Faculty of Science, Menofia University, Cairo, Egypt

Several methods have been reported so far for the synthesis of gold NPs and their alloys with other NPs to produce gold-metal core/shell structures. Pulsed laser ablation of targets in liquid environment (PLAL) is one of these methods and it has been studied intensely during the past decade. PLAL reduces the formation of by-product, its setup is very simple, and it does not need catalyst or complicated requirements to make purification [14, 15]. PLAL provides efficient technique for the synthesis of size and shape controllable metallic and bimetallic NPs in colloidal solution. Nonetheless, according to the importance of nanocomposites and a simple method several scientific groups focused on study of the interaction between metals and laser irradiation. There are large numbers of PLAL parameters used to control the shape, size, and morphology of NPs which can be divided to laser parameters and solution medium parameters. The laser parameters are wavelength, pulse width, laser energy, repetition rate, and ablation time. The solution medium parameters are composition, dipole moment, dielectric constant, and absorption constant [16–19]. Almost typical works of bimetallic of gold metal and another metal in recent years are summarized in Table 1 [20–30].

Year	Research group	Product	Target	Liquid medium	Laser type, wavelength, pulse duration, frequency, fluence (or energy per pulse), ablation time (or pulse number), notes	Number of steps	Product (size)	Surface Plasmon Resonance (SPR)
2015	Suzana Petrovi et al. [19]	Au–Ni NPs	Ni	Colloidal Au solution concentration of 0.2 mmol d/m^3 with nanoparticles of about 5 nm size	Two Nd:YAG lasers: one with the pulse width of 20 ns, and another with the pulsewidth of 150 ps. Both lasers 10 Hz, $\lambda = 1064$ nm, 10 mJ, 50 and 20 min for nanosecond and picosecond pulses, respectively	1	5–7 nm	520 nm
	K.G. Gopchandran et al. [20]	Ag–Au core shell	Au/Ag targets	20 ml of double distiled water at room temperature	Nd:YAG, $\lambda = 1064$ nm, 10 Hz, low energy	2	11–16 nm	519 and 413 nm
	Zahra Sheykhifard et al. [21]	Au–Pd (II) core shell	Au	0.02 g of $PdCl_2$ solution, DI water, and 0.1 mL HCl	Nd:YAG, $\lambda = 1064$ nm, 10 Hz, 360 mJ, 1 h	1	7–12 nm	530 nm
	Dongling Ma et al. [22]	PtAu Alloy NPs	PtAu Alloy	Aqueous solution (pH = 4.0–11.0)	KrF excimer laser, $\lambda = 248$ nm, exciting voltage: 37 kV, 20 Hz. 4.0–150.0 J/cm^2	1	3.5 ± 1.6 nm	
2012	Koshizaki et al. [23]	Au/AuFe	Au plate	Ethanol	Nd:YAG, $\lambda = 1064$ nm, 30 Hz, and 80 J/pulse cm^2 fluence	2	5 nm	528 nm

Year	Research group	Product	Target	Liquid medium	Laser type, wavelength, pulse duration, frequency, fluence (or energy per pulse), ablation time (or pulse number), notes	Number of steps	Product (size)	Surface Plasmon Resonance (SPR)
2011	Pietro Calandra et al. [24]	Au/TiO2 NPs	Au target	Water	Nd:YAG, $\lambda = 532$ nm, plse width 5 ns, 10 Hz, 120 mJ	2	< 50 nm	470
	Geetika Bajaj et al. [25]	Au–Sn oxide NPs	Au plate	DI water	Nd:YAG, $\lambda = 532$ nm, 10 Hz, (Au:36 mJ, 15 min, Sn: 18 mJ, 30 min) then the mixture was irradiated with Nd:YAG, $\lambda = 532$ or 1064 nm	2	8–26 nm	532
2010	Geetika Bajaj et al. [26]	Au–Sn oxide NPs	Au plate	DI water	Nd:YAG, $\lambda = 532$ nm, 10 Hz, 4.6 J/cm2, 1 h	2	15 nm	520 nm
	Michel Meunier et al. [27]	Au–Ag alloy NPs	Au and Ag targets	Dextran solution	Ti:sapphire laser, $\lambda = 800$ nm, pulse width 110 fs,1 kHz, 0.3 J/cm^2	2	Au and Ag NPs are 3.3 ± 1.5 and 4.4 ± 2.7 nm, respectively	398:520 nm
	Michel Meunier et al. [28]	Au–Co alloy NPs	Au and Co targets	Acetone	Ti:sapphire laser, $\lambda = 800$ nm, pulse width 120 fs, 0.9 mJ/pulse, 10 kHz, 60 min	2	11 nm	520 nm
2004	G.A. Shafeev et al. [29]	Au–Ag alloy NPs	Au and Ag plates	Ethanol or distilled water ad PVP	Cu vapor laser, $\lambda = 510.6$ nm, pulse width 20 ns, 7.5 kHz, 9 J/cm^2, 2 steps	2	10 nm	400:550 nm

In this paper, bimetallic structure from Au and Cd as a Au@CdO core/shell NPs are fabricated for the first time in just one step without using any surfactant. Nd-YAG Pulse laser with 7 ns is used to ablate a Cd sheets solid target in a solution containing gold precursors. The structural, compositional and optical properties of Au@CdO core/shell NPs obtained using UV–VIS, TEM, XRD, FT-IR, and EDX analyses techniques on the colloid samples. In addition, a proposal of the possible mechanism of fabrication bimetallic structure from Au and Cd as a Au@CdO core/shell is investigated.

2 Experimental section

2.1 Materials

Cd metal granulated sheets (≥ 99.9%) were purchased from BDH chemical Ltd pool, England. Chloroauric acid ($HAuCl_4 \bullet 3H_2O$) was obtained from Sigma–Aldrich Co. All reagents were analytical grade and used without further purification. Water was purified by a Millipore Ultrapure water system and has a resistivity of 18.2 MΩ cm at 25 °C.

2.2 Preparation of Colloids by PLAL

A novel Au@CdO core/shell NPs were prepared in just one step as follow: Cleaned Cd sheets were immersed in 5 ml solution of de-ionized water containing 1 ml solution of (5×10^{-5}M) $HAuCl_4$. The Cd sheet target was irradiated with the 2nd harmonic of pulsed Nd:YAG laser operating at 1064 nm with pulse repetition rate 10 Hz, pulse width 7 ns, and laser energy 80 mJ/pulse. The laser beam was focused on the target surface using a lens of focal length 70 mm. The ablation was carried out for 10 min (see Fig. 1). The depth of the solution layer above the target was 10 mm. During this process, the solution was stirred by mechanical rotator to enhance the growth of the produced NPs [16]. Finally, the colloidal Au@CdO core/shell NPs were obtained.

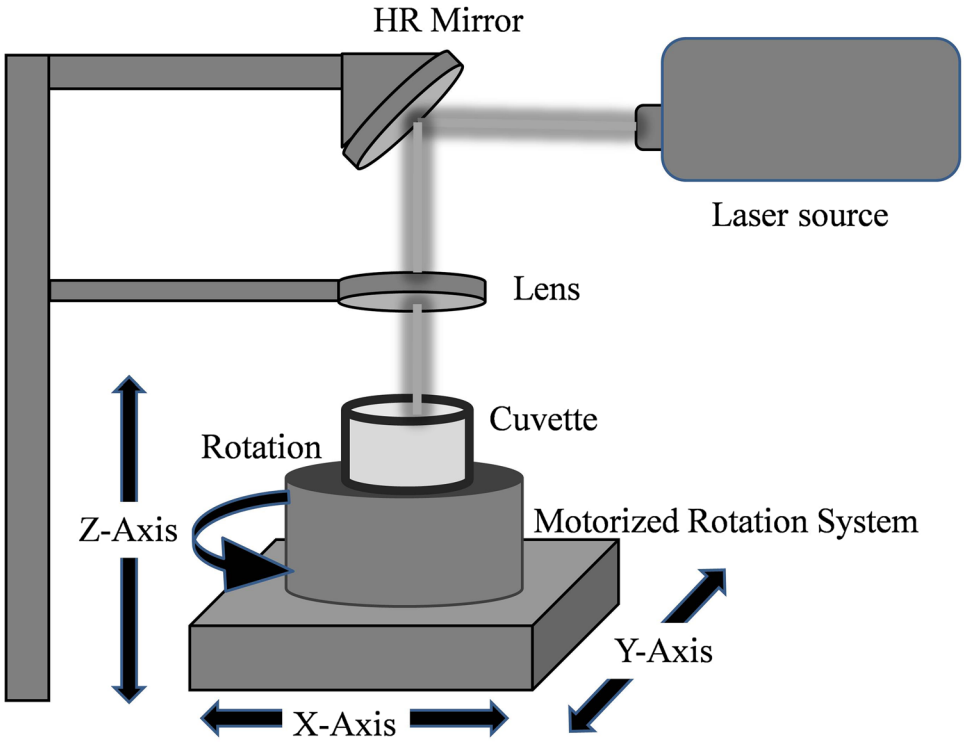

Fig. 1 Schematic representation of Pulsed laser ablation in liquid technique

2.3 Characterization techniques

Optical properties of samples were measured in the 190–1000 nm wavelength range using quartz cells with 1 cm optical path length using a JASCO 570 UV-VIS-NIR spectrophotometer, Japan.

The crystalline structure of samples was characterized using X-ray (XRD) diffractometer (Schimadzu 7000, Japan) operating with Cu Kα radiation ($\lambda = 0.154060$ nm) generated at 30 kV and 30 mA with scanning rate of 4°/min for 2θ values between 10° and 80°.

The size and shape of NPs were observed on a high resolution transmission electron microscope (HRTEM) of the type JEOL—JEM-1011, Japan. Scan images were recorded at accelerated voltage of 200 kV. For each sample, a drop of low concentrated NPs suspension was deposited on a copper grid covered by carbon layer. The excess solution was wicked by a filter paper and the grid was left to dry at room temperature for 12 h.

A Fourier-transform infrared spectroscopy (JASCO FT/IR 6100 spectrometer, 64 scans with 4 cm^{-1} resolution) was employed to demonstrate the chemical composition of nanomaterials in the range of 4000–400 cm^{-1}. The prepared sample was mixed with potassium Bromide (KBr) for the extent of OH signature.

Energy dispersive X-ray spectroscopy (EDX) measurements were also performed on single particles for chemical analysis using scanning electron microscopy on a Quanta FEG 250 electron microscope.

ImageJ software has been pioneers as open tools for the analysis of scientific images to stimulate the ultra-structural TEM and SEM analysis reader to solve common tasks in laboratory practice.

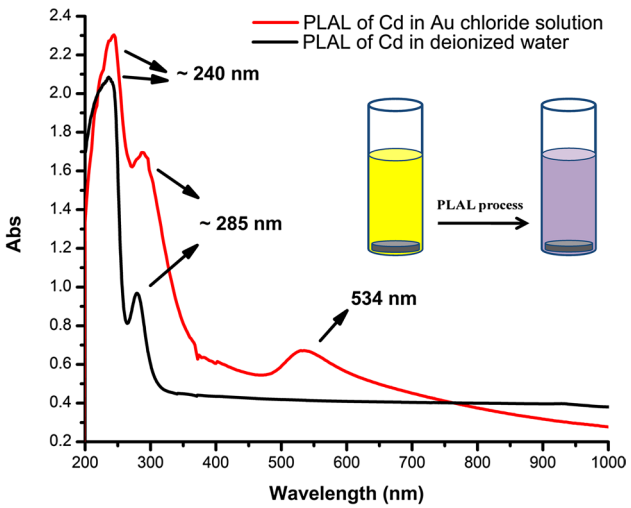

Fig. 2 UV-Visible absorption spectra of Au-Cd NPs fabricated by PLAL

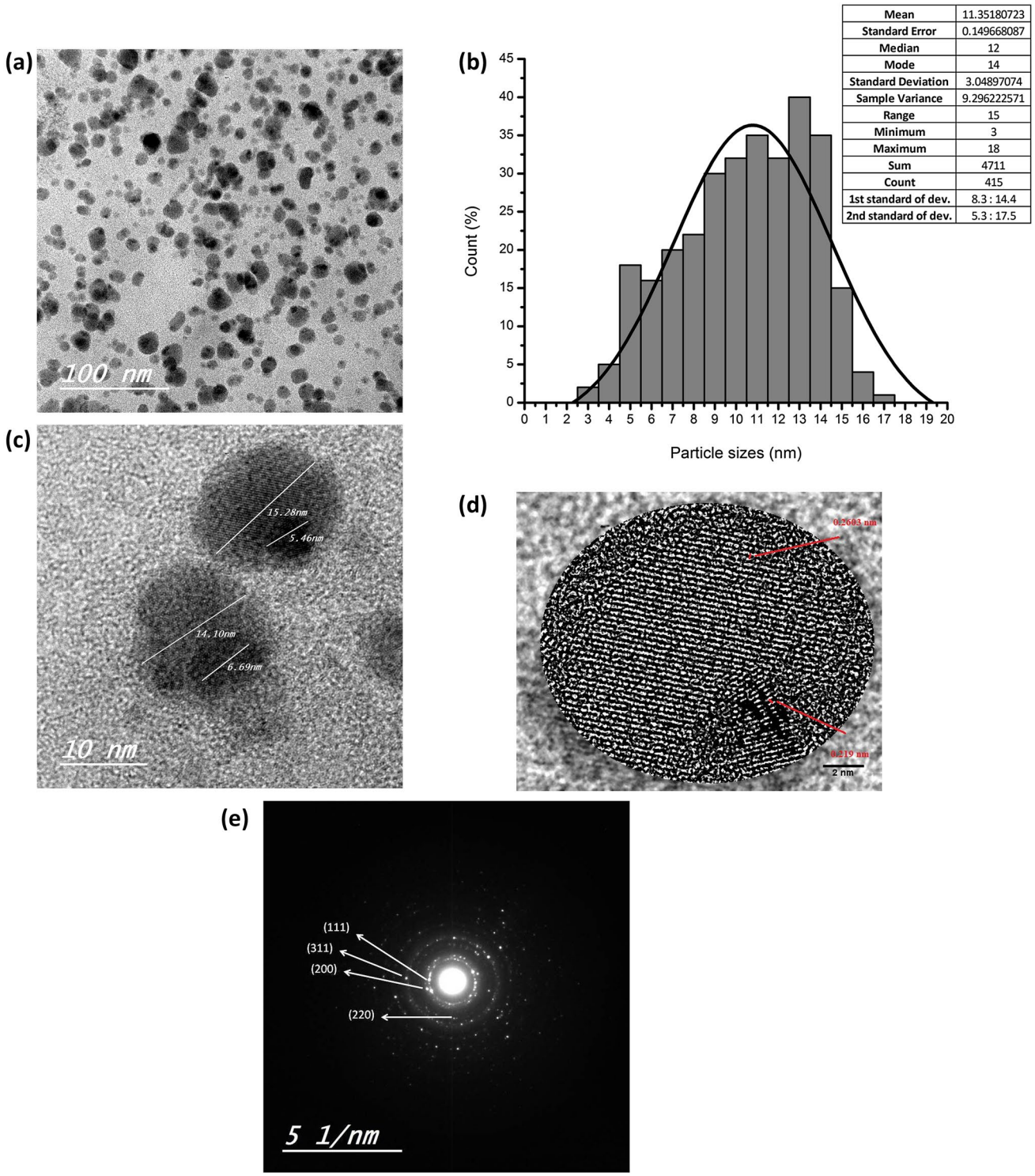

Mean	11.35180723
Standard Error	0.149668087
Median	12
Mode	14
Standard Deviation	3.04897074
Sample Variance	9.296222571
Range	15
Minimum	3
Maximum	18
Sum	4711
Count	415
1st standard of dev.	8.3 : 14.4
2nd standard of dev.	5.3 : 17.5

Fig. 3 **a** TEM image of Au-Cd NPs produced by PLAL @100nm. **b** TEM histogram of Au@CdO NPs @100nm. **c** TEM image of Au@CdO NPs @10nm. **d** The inter planner distance calculation of Au@CdO. **e** The selected area diffraction (SAED) pattern

3 Results and discussion

3.1 UV–VIS analysis

The effect of nanosecond pulsed laser ablation of Cd sheet target in deionized water and $HAuCl_4$ solution were primarily followed with the naked eye. The ablation of Cd sheet in deionized water (DI) yielded a pale white color while the ablation in $HAuCl_4$ resulted in color conversion of the solution from yellow to deep violet color. This observation can be illustrated using UV–vis absorption analysis.

Figure 2 shows the UV–vis spectra of the ablated Cd sheet in DI water as compared with that ablated in $HAuCl_4$ solution. The absorption spectrum of the ablated Cd sheet in DI water showed two absorption peaks at ~ 240 and ~ 285 nm. The electronic band at ~ 240 nm was attributed to inter-band transition from deep level electrons of VB while the signal at ~ 285 nm was related to quantum confinement effect [18, 31]. The UV–vis spectrum of the Cd sheet ablated in $HAuCl_4$ solution showed a new absorption band at 534 nm in addition to the two preceding absorption peaks i.e. 240 and 285 nm. The absorption peak at 534 nm is consistent with the appearance of the violet color. This absorption peak was attributed to the SPR band of the gold NPs. It should be noted that the exposure of the $HAuCl_4$ solution in absence of Cd sheet did not yield any color changes. Hence, it could be concluded that the presence of ablated Cd ions are essential for the reduction of Au NPs.

3.2 TEM analysis

To get more precise view of the detailed structure of the prepared nanocomposite, HRTEM was used. Figure 3 shows the HRTEM images and corresponding size distribution histogram of Au/CdO NPs sample. Figure 3a showed a number of semi-spherical particles with color gradient i.e. black core surrounded with grey shell. This color gradient was attributed to the difference of the electron density between Au (atomic number = 79) and Cd (atomic number = 48). Hence, the black core was attributed to the Au NPs and the grey color was attributed to the CdO shell. The particles are separated from each other and less number of aggregations was observed within field image. For that the Au core is eccentric with respect to the surrounding CdO shell due to a retarded $AuCl_4$ reduction with respect to the NPs CdO formation, i.e. the Au growth needs the formation of a CdO surface to start. According to the size distribution histogram (Fig. 3b) of this sample the average particle size of core/shell is about 11.35 nm with 1st standard of deviation from 8.3:14.4 nm and 2nd standard of deviation from 5.3:17.5 nm.

Figure 3c is made by focusing on the CdO shell and the Au core. The image clearly showed that both the CdO shell and the Au core are single crystalline materials. The interplanar distance between the adjacent lattice fringes can be determined using ImageJ software (open access) as shown in Fig. 3d. In this figure, 10 lattice fringes of core and shell were measured, followed by calculation of mean lattice fringes of core (Au NPs) and shell (CdO NPs) to be 0.219 and 0.2603 nm, respectively. Further, the selected area diffraction (SAED) pattern in Fig. 3e indicates that the grown particles are crystalline in nature and have FCC lattice.

3.3 FTIR analysis

The FTIR spectrum of the representative sample is shown in Fig. 4. The spectrum showed the broad peak at region between 3000 to 3600 cm^{-1} (OH stretching mode) and 1631 cm^{-1} (H_2O bending mode) due to the free and

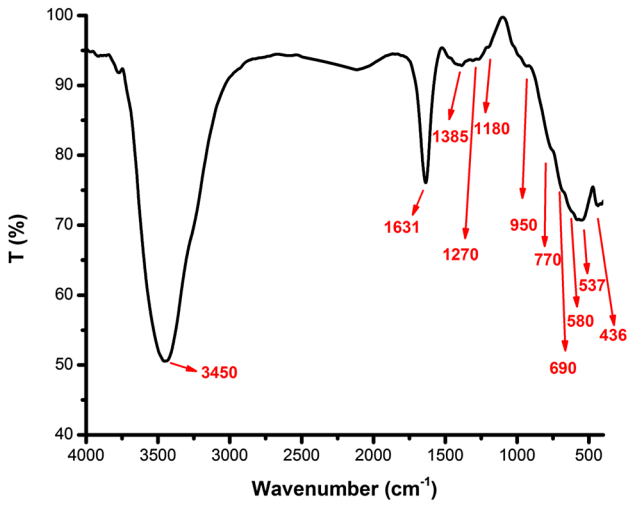

Fig. 4 FTIR spectra of Au-Cd NPs fabricated by PLAL

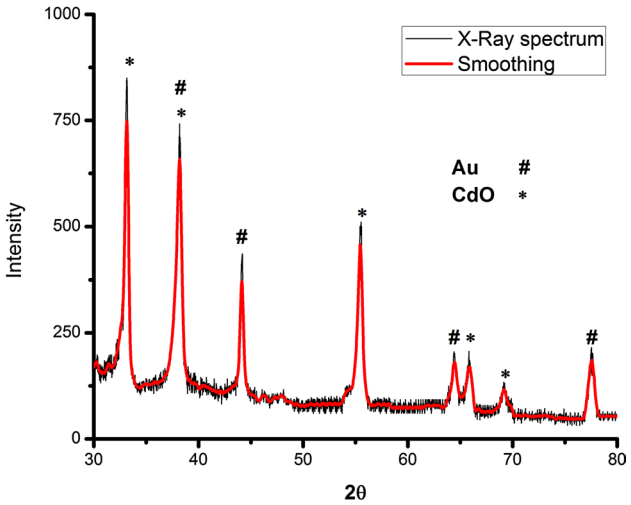

Fig. 5 X-ray diffraction pattern of Au-Cd NPs fabricated by PLAL

hydrogen bonded of O-H hydroxyl group stretching bond of water absorbed molecule on the powder surface. These functional groups of OH and H_2O could be appeared due to water adsorbed on NPs surface or from atmospheric water vapor phase [32–35]. According to the transmittance peaks between 800 and 1500 cm^{-1} assigned to CdO [34], the transmittance band at 1385, 1270, and 1180 cm^{-1} can be assigned as bending and wagging vibrations motion of the formed metal oxide structure [32]. The band at 690, 580, 537, and 436 cm^{-1} is correlated to the formation of Cd–O [36–38].

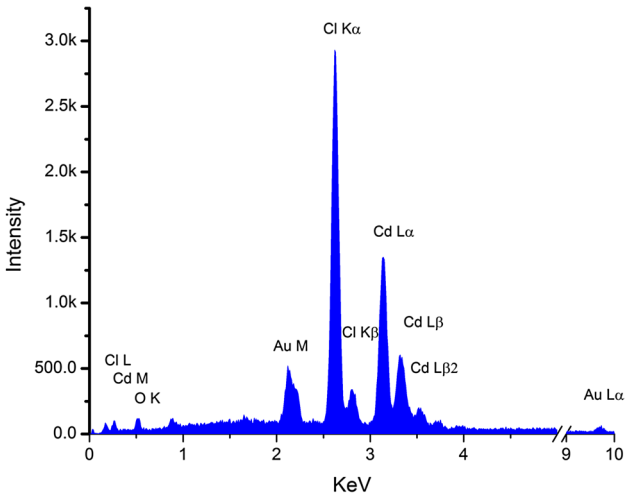

Fig. 6 EDX elemental analysis of Au@CdO NPs

3.4 X-ray diffraction

Figure 5 shows the powder XRD patterns of nanostructures prepared by PLAL. It is clear that the more remarkable peaks were observed at $2\theta = 33.16^{\circ}$, 38.16°, 44.06°, 55.19°, 64.41°, 65.86°, 69.15°, and 77.56°. The discernible peaks of 38.16 °, 44.06 °, 64.41 °, and 77.56 ° can be, respectively, indexed to (111), (200), (220), and (311) planes of the face-centered structure of Au according to the lattice constants close to the values in previous literatures (JCPDS no. 65-2870). On the other hand, the diffraction peaks existed at 33.16°, 38.16°, 55.19°, 65.86°, and 69.15° can be, respectively, indexed to (111), (200), (220), (311), and (222) planes of face-centered structure of CdO according to the lattice constants close to the values in previous literatures (JCPDS no. 75–0592). In addition, No diffraction peaks of metallic Cd appeared in X-Ray diffraction patterns of samples, indicating that the metallic Cd phase might exist in an amorphous phase (not well crystalline phase) or in the form of very small clusters.

3.5 EDX

EDX spectra were collected for at least 30 measurements at randomly chosen position. Figure 6 shows the presence of Cd and Au on the surface as the following amounts 27% of Cd and 24% of Au. All of that beside the amount of Cl is remaining without reaction from the starting materials of $HAuCl_4$.

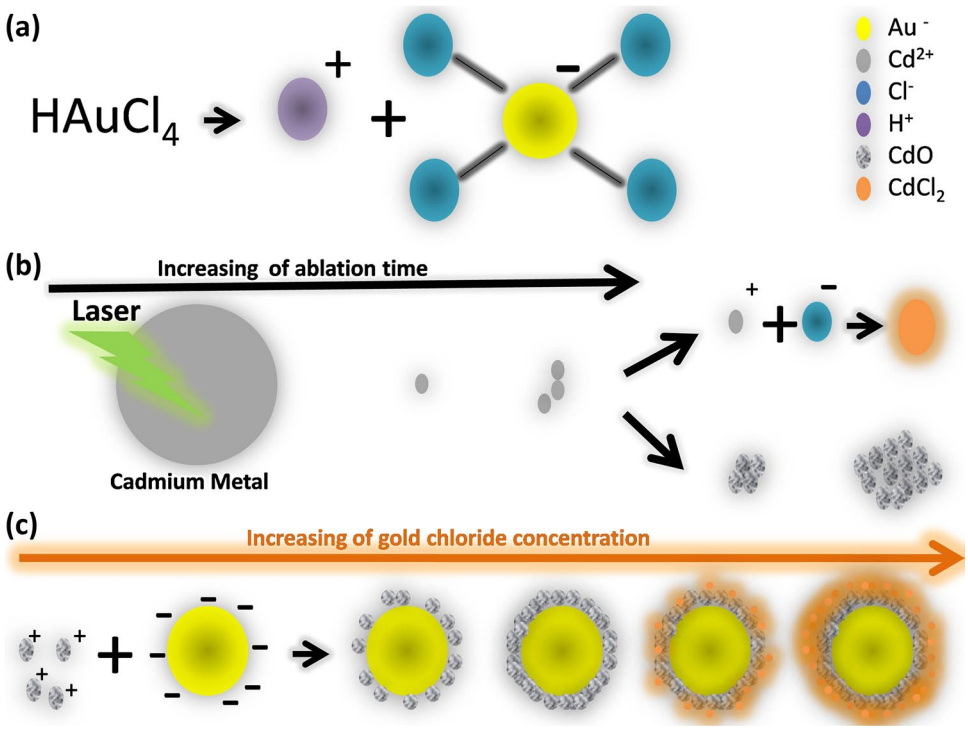

Fig. 7 Schematic model for **a** dissociation of HAuCl4 **b** Cd sheets journey in thelaser-matter interaction by increasing the time of ablation **c** Cd and Au interaction by

Further, the mapping of Au@CdO NPs studied in Fig. 7 indicates that the Au@CdO NPs is prepared well.

4 Mechanism

At the very early stages of the laser/Cd interaction, species ejected from the Cd sheet surface with high kinetic energy forming a dense cloud nearby the solid/liquid interface due to the confinement effect of liquid. It was reported that this cloud contains a mixture of reducing species such as electrons, ions, and free radicals [39, 40]. Our experimental observations and the UV–VIS results showed that no change occurred in the solution color when irradiation was carried out in absence of Cd sheet i.e. the laser beam was unable to reduce Au^{3+} to Au NPs.

These results might enforce to believe that the Cd species were responsible for the reduction of Au ions. This reduction reaction could be attributed to the well known galvanic replacement. The galvanic replacement reaction is considered as a redox process. This process draw the driving force from the difference between the reduction potential (E°) of the two reactants. Since E° $AuCl_4^-$/Au pair (0.99 V) is higher than that of the Cd^{2+}/Cd pair (−0.40 V) [41], the following reaction would happen in the solution:

$$3Cd^{0}_{(s)} + 2AuCl_{4(aq)}^{-1} \rightarrow 2Au^{0}_{(s)} + 3Cd^{+2}_{(aq)} + 8Cl^{-1}_{(aq)}$$

After ablation of Cd sheet, Au^{3+} ions were reduced by Cd to form Au atoms. As the reaction went on, Au nuclei formed and subsequently the Au NPs grew.

Moreover, Because the noble metals NPs have high negative charge compared to other metals, Therefore, the Au NPs could attract the other metals (In this case Cd^{2+}). Therefore the surface of Au cores is assumed to have a deterministic role for an ability to trap Cd ions owing to surface negative charges. So, the alloy or core/shell structure is produced in nanoscale [22]. According to thermodynamic state of PLAL from high pressure, temperature, and density, the oxidation process during laser ablation in water has been done [41–43]. This oxidation process during laser synthesis is mainly caused by reactive oxygen species from the decomposition of water molecules. Using this consideration, Cd ions react with activated oxygen and form a CdO shell. A schematic model that summarizes the discussion is shown in Fig. 7.

5 Conclusions and perspectives

Au@CdO core/shell nanostructure was successfully fabricated for first time using green method of pulsed laser ablation in liquid environmental (PLAL) in just one step. This work can be represented a new way to fabricate a lot of binary compound as alloying or core/shell structure in nanoscale. The techniques of XRD, UV–Vis, FT-IR, HRTEM, and EDAX confirm that the suspension solution is well fabricated as Au@CdO core/shell NPs with average diameter about 11 nm. The mechanism of synthesis Au@CdO core/shell NPs is studied based on study three main steps: (a) laser-matter interactions of PLAL process (representative of first metal of core/shell), (b) dissociation of gold salt in aqueous solution (representative of secondary metal of core/shell), and (c) formation of Au@CdO core/shell NPs based on galvanic replacement reaction phenomena.

Acknowledgements This paper draws on work supported by the facilities of Laser Technology Unit, National Research Centre, Egypt.

References

1. S. Horikoshi, N. Serpone, *Microwaves in Nanoparticle Synthesis: Fundamentals and Applications*. (John Wiley, Berlin, 2013)
2. E.A. Mwafy, A.A. Abd-Elmgeed, A.A. Kandil, I.A. Elsabbagh, M.M. Elfass, M.S. Gaafar, High UV-shielding performance of zinc oxide/high-density polyethylene nanocomposites. Spectrosc. Lett. **48**(9), 646–652 (2015)
3. A. Abou-Kandil, A. Awad, E Mwafy, Polymer nanocomposites part 2: optimization of zinc oxide/high-density polyethylene nanocomposite for ultraviolet radiation shielding. J. Thermoplast. Compos. Mater. **28**(11), 1583–1598 (2015)
4. V. Abdelsayed, G. Glaspell, M. Nguyen, J. Howe, M. El-Shall, Laser synthesis of bimetallic nanoalloys in the vapor and liquid phases and the magnetic properties of Pdm and Ptm nanoparticles (M = Fe, Co and Ni). Faraday Discuss **138**, 163–180 (2008)
5. N. Toshima, Core/shell-structured bimetallic nanocluster catalysts for visible-light-induced electron transfer. Pure Appl. Chem. **72**(1–2), 317–325 (2009)
6. J. Liao, Y. Zhang, W. Yu, L. Xu, C. Ge, J. Liu, N. Gu, Linear aggregation of gold nanoparticles in ethanol. Colloids Surf. A 223, 177–183 (2003)
7. S. Stadnichenko, A. Koshcheev, Boronin, Oxidation of the polycrystalline gold foil surface and Xps study of oxygen states in oxide layers. Moscow Univ. Chem. Bull. **62**(6), 343–349 (2007)
8. W.M. Darwish, A.M. Darwish, E.A. Al-Ashkar, Indium(III) phthalocyanine eka-conjugated polymer as high-performance optical limiter upon nanosecond laser irradiation. High Perform. Polym. **28**(6), 651–659 (2016)
9. W.M. Darwish, A.M. Darwish, E.A. Al-Ashkar, Synthesis and nonlinear optical properties of a novel indium pthalocyanine highly branched polymer. Polym. Adv. Technol. **26**(8), 1014–1019 (2015)
10. C.T. Nguyen, J.T. Nguyen, S. Rutledge, J. Zhang, C. Wang, G.C. Walker, Detection of chronic lymphocytic leukemia cell surface markers using surface enhanced Raman scattering gold nanoparticles. Cancer Lett. **292**, 91–97 (2010)
11. M.L. Pacea, A. Guarnaccioa, F. Ranùa, D. Trucchib, S. Orlandoa, D. Mollicaa, G.P. Parisia, L. Medicic, A. Lettinoc, A. De Bonisd, R. Teghild, A. Santagataa, Plasmonic angular tunability of gold nanoparticles generated byfs laser ablation. Appl. Surf. Sci. **374**, 397–402 (2016)

12. V. Amendola, S. Scaramuzza, S. Agnoli, S. Polizzi, M. Meneghetti, Strong dependence of surface plasmon resonance and surface enhanced raman scattering on the composition of Au–Fe nanoalloys. Nanoscale **6**, 1423–1433 (2014)
13. M. Tadjarodi, Imani, A novel nanostructure of cadmium oxide synthesized by mechanochemical method. Mater. Res. Bull. **46**, 1949–1954 (2011)
14. F. Mafune, J.-Y. Kohno, Y. Takeda, T. Kondow, H. Sawabe, Formation and size control of silver nanoparticles by laser ablation in aqueous solution. J. Phys. Chem. B **104**, 9111–9117 (2000)
15. J. Zhang, M. Post, T. Veres, Z.J. Jakubek, J. Guan, D. Wang, F. Normandin, Y. Deslandes, B. Simard, Laser-assisted synthesis of superparamagnetic Fe@Au core/shell nanoparticles. J. Phys. Chem. B, **110**, 7122–7128 (2006)
16. M. Darwish, W.H. Eisa, A.A. Shabaka, M.H. Talaat, Investigation of factors affecting the synthesis of nano-cadmium sulfide by pulsed laser ablation in liquid environment. Spectrochim. Acta Part A Mol. Biomol. Spectrosc. **153**, 315–320 (2016)
17. M. Darwish, W.H. Eisa, A.A. Shabaka, M. H. Talaat, Synthesis of nano-cadmium sulfide by pulsed laser ablation in liquid environment. Spectrosc. Lett. **48** (9), 638–645 (2015)
18. M. Mostafa, S.A. Yousef, W.H. Eisa, M.A. Ewaida, E.A. Al-Ashkar, Synthesis of Cadmium Oxide Nanoparticles by pulsed laser ablation in liquid environment. Optik-Int. J. Light Electron Optics **144**, 679–684 (2017)
19. R.M. Tilaki, A. Irajizad, S.M. Mahdavi, Stability, size and optical properties of silver nanoparticles prepared by laser ablation in different carrier media. Appl Phys A **84**, 215–219 (2006)
20. D. Suzana Petrovi, B. Milovanov, D. Salat, J. Peru_sko, G. Kova, M. Dra_zi, M. Mitri, B. Trtica, Jelenkovi, Composition and structure of NiAu nanoparticles formed by laser ablation of Ni target in Au colloidal solution. Mater. Chem. Phys. **166**, 223–232 (2015)
21. M. Vinod, K.G. Gopchandran, Ag@Au core–shell nanoparticles synthesized by pulsed laser ablation in water: effect of plasmon coupling and their SERS performance. Spectrochim. Acta Part A Mol. Biomol. Spectrosc. **149**, 913–919 (2015). https://doi.org/10.1016/j.saa.2015.05.004
22. Z. Sheykhifard, M. Ranjbar, H. Farrokhpour, H. Salamati, Direct Fabrication of Au/Pd(II) colloidal core-shell nanoparticles by pulsed laser ablation of gold in PdCl2 solution. J. Phys. Chem. C **119**, 9534–9542 (2015)
23. J. Zhang, D. Nii Oko, S. Garbarino, R. Imbeault, M. Chaker, A.C. Tavares, D. Guay, D. Ma, Preparation of PtAu alloy colloids by laser ablation in solution and their characterization. J. Phys. Chem. C **116**(24), 13413–13420 (2012)
24. Z. Swiatkowska-Warkocka, K. Kawaguchi, Y. Shimizu, A. Pyatenko, H. Wang, N. Koshizaki, Synthesis of Au-based porous magnetic spheres by selective laser heating in liquid. Langmuir **28**, 4903–4907 (2012)
25. E. Fazioa, P. Calandrab, V. Turco Liveri, N. Santod, S. Trusso, Synthesis and physico-chemical characterization of Au/TiO_2 nanostructures formed by novel "cold" and "hot" nanosoldering of Au and TiO_2 nanoparticles dispersed in water. Colloids Surf. A Physicochem. Eng. Aspects **392**, 171–177 (2011)
26. G. Bajaj, R.K. Soni, Gold/tin oxide nanocomposite by nanojoining. Open Surf. Sci. J. **3**, 65–69 (2011)
27. G. Bajaj, R.K. Soni, Synthesis of composite gold/tin-oxide nanoparticles by nano-soldering. J. Nanopart. Res. **12**(7), 2597–2603 (2010)
28. S. Besner, M. Meunier, Femtosecond laser synthesis of AuAg nanoalloys: photoinduced oxidation and ions release. J. Phys. Chem. C **114**(23), 10403–10409 (2010)
29. P. Boyer, D. Me´nard, M. Meunier, Nanoclustered Co-Au particles fabricated by femtosecond laser fragmentation in liquids. J. Phys. Chem. C **114**(32), 13497–13500 (2010)
30. T. Izgaliev, A.V. Simakin, G.A. Shafeev, F. Bozon-Verduraz, Intermediate phase upon alloying Au–Ag nanoparticles under laser exposure of the mixture of individual colloids. Chem. Phys. Lett. **390**, 467–471 (2004)
31. S. Kumar, A.K. Ojha, B. Walkenfort, Cadmium oxide nanoparticles grown in situ on reduced graphene oxide for enhanced photocatalytic degradation of methylene blue dye under ultraviolet irradiation. J. Photochem. Photobiol. B Biol. **159**, 111–119 (2016)
32. E. Solati, M. Mashayekh, D. Dorranian, Effects of laser pulse wavelength and laser fluence on the characteristics of silver nanoparticle generated by laser ablation. Appl. Phys. A Mater. Sci. Process **112**, 689–694 (2013)
33. R.B. Fahim, G.A. Kolta, Thermal decomposition of hydrated cadmium oxide. J. Phys. Chem **74**(12), 2502–2506 (1970)
34. K. Kaviyarasu, E. Manikandan, P. Paulraj, S.B. Mohamed, J. Kennedy, One dimensional well-aligned CdO nanocrystal by solvothermal method. J. Alloy Compd. **593**, 67–70 (2014)
35. S. Gandhi, R.H.H. Subramani, T. Ramankrishnan, A. Sivabalan, V. Dhanalakshmi, M.R.G. Gopinath Nair, R. Anbarasan, Ultrasound assisted one pot synthesis of nano-sized CuO and its nanocomposite with poly (vinyl alcohol). J. Mater. Sci **45**, 1688–1694 (2010)
36. K. Kaviyarasu, C. Maria Magdalane, K. Anand, E. Manikandan, M. Maaza, Synthesis and characterization studies of MgO:CuO nanocrystals by wet-chemical method. Spectrochim. Acta Part A **142**, 405–409 (2015)
37. S. Sivakumar, A. Venkatesan, P. Soundhirarajan, C.P. Khatiwada. Synthesis, characterizations and anti-bacterial activities of pure and Ag doped CdO nanoparticles by chemical precipitation method. Spectrochim. Acta Part A Mol. Biomol. Spectrosc. **136**, 1751–1759 (2015)
38. D. Moses Ezhil Raj, V. Deva Jayanthi, Bena Jothy, Optimized growth and characterization of cadmium oxalate single crystals in silica gel. Solid State Sci **10**(5), 557–562 (2008)
39. T. Kaneko, K. Baba, R. Hatakeyama, Static gas-liquid interfacial direct current discharge plasmas using ionic liquid cathode. J. Appl. Phys. **105**(10), 103306 (2009)
40. M. Mostafa, M.F. Hameed, S.S. Obayya, Effect of laser shock peening on the hardness of AL-7075 alloy. J. King Saud. Univ. Sci. (2017). https://doi.org/10.1016/j.jksus.2017.07.012
41. P.W. Atkins, P.W. Atkins, *The Elements of Physical Chemistry*, vol. 496 (Oxford University Press, Oxford, 1992)
42. Z. Liu, Y. Yuan, S. Khan, A. Abdolvand, D. Whitehead, M. Schmidt, L. Li, Generation of metal-oxide nanoparticles using continuous-wave fibre laser ablation in liquid. J. Micromech. Microeng. **19**(5), 1–7 (2009)
43. P. Maneeratanasarn, T. Van Khai, S.Y. Kim, B.G. Choi, K.B. Shim, Synthesis of phase-controlled iron oxide nanoparticles by pulsed laser ablation in different liquid media. Phys. Status Solidi. A **210**(3), 563–569 (2013)